JOC Article

Dynamic Chirality in Donor−Acceptor Pretzelanes

Y. Liu,† S. A. Vignon, X. Zhang, P. A. Bonvallet,‡ S. I. Khan, K. N. Houk, and J. F. Stoddart*

California NanoSystems Institute and Department of Chemistry and Biochemistry, University of California, Los Angeles, 405 Hilgard Avenue, Los Angeles, California 90095-1569

stoddart@chem.ucla.edu

Received July 11, 2005

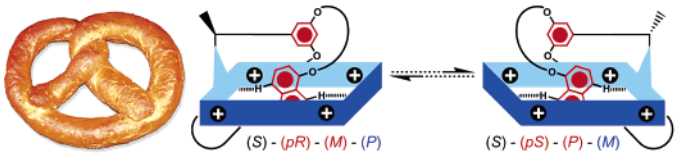

A series of donor−acceptor pretzelanes has been synthesized, using self-assembly and template-directed protocols, and the dynamic processes that these pretzelanes undergo have been investigated in solution. These compounds exist as libraries of diastereoisomers as a result of their multiple stereoelements, which are dynamically interconverted by several different, in some cases competing, processes. Altering the structure of the pretzelanes changes the rates and mechanisms by which these diastereoisomers equilibrate. Additionally, inserting an element of fixed chirality allows the equilibrium to be biased, while maintaining the barrier to the equilibration processes. These results bode well for the future construction of molecular devices based on switchable diastereoisomerism involving metastable states.

Introduction

Investigations into the nature of mechanically interlocked compounds[1] have become increasingly prevalent with the development of self-assembly[2] and template-directed[3] protocols in synthesis. Some of the structural motifs studied include catenanes,[4] rotaxanes,[4] knots,[4,5] and Borromean links.[6] These compounds consist of one or more molecular components linked together by mechanical bonds. Noncovalent interactions, such as hydrogen bonding and donor−acceptor interactions that drive the assembly of these systems, persist in the interlocked molecules, affecting the co-conformations adopted by them. As a result, many of these mechanically interlocked compounds possess interesting dynamic processes and stereochemical elements. Extensive investigations[7] have been carried out to understand these phenomena and their potential applications for the creation of molecular machines[8] and switches.[9]

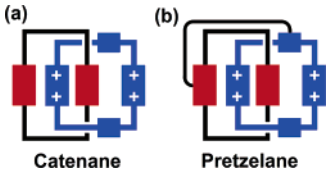

FIGURE 1. Schematic representation of a (a) [2]catenane and (b) a pretzelane.

Pretzelanes (Figure 1), or bridged [2]catenanes, have also been studied extensively in recent years. The first pretzelanes were synthesized[10] by Vögtle, starting from sulfonamide-based macrocycles and catenanes. Chiral versions of these hydrogen bonded pretzelanes were also synthesized[11] by introducing directionality into the con-

* Address correspondence to this author. Fax: (+1) 310-206-1843.
† Current address: Department of Chemistry, BCC-315, The Scripps Research Institute, 10550 North Torrey Pines Road, La Jolla, CA 92037.
‡ Current address: Department of Chemistry, College of Wooster, 943 College Mall, Wooster, OH 44691.

(1) Amabilino, D. B.; Stoddart, J. F. *Chem. Rev.* **1995**, *95*, 2725−2828.
(2) (a) Lindsey, J. S. *New J. Chem.* **1991**, *15*, 153−180. (b) Philp, D.; Stoddart, J. F. *Angew. Chem., Int. Ed. Engl.* **1996**, *35*, 1154−1196. (c) Fujita, M. *Acc. Chem. Res.* **1999**, *32*, 53−61. (d) Rebek, J., Jr. *Acc. Chem. Res.* **1999**, *32*, 53−61. (e) Bong, D. T.; Clark, T. D.; Granja, J. R.; Ghadiri, M. R. *Angew. Chem., Int. Ed.* **2001**, *40*, 988−1011. (f) Prins, L. J.; Reinhoudt, D. N.; Timmerman, P. *Angew. Chem., Int. Ed.* **2001**, *40*, 2382−2426. (g) Seidel, S. R.; Stang, P. J. *Acc. Chem. Res.* **2002**, *35*, 972−983. (h) Reinhoudt, D. N.; Crego-Calama, M. *Science* **2002**, *295*, 2403−2407.
(3) (a) *Templated Organic Synthesis*; Diederich, F., Stang, P. J., Eds.; Wiley-VCH: Weinheim, Germany, 1999; (b) Stoddart, J. F.; Tseng, H.-R. *Proc. Natl. Acad. Sci. U.S.A.* **2002**, *99*, 4797−4800. (c) Aricó, F.; Badjic, J. D.; Cantrill, S. J.; Flood, A. H.; Leung, K. C.-F.; Liu, Y.; Stoddart, J. F. *Top. Curr. Chem.* **2005**, *249*, 203−259.
(4) *Molecular Catenanes, Rotaxanes and Knots*; Sauvage, J.-P., Dietrich-Buchecker, C., Eds.; Wiley-VCH: Weinheim, Germany, 1999.
(5) (a) Sauvage, J.-P. *Acc. Chem. Res.* **1990**, *23*, 319−327. (b) Ashton, P. R.; Matthews, O. A.; Menzer, S.; Raymo, F. M.; Spencer, N.; Stoddart, J. F.; Williams, D. J. *Liebigs Ann.* **1997**, 2485−2494. (c) Lukin, O.; Vögtle, F. *Angew. Chem., Int. Ed.* **2005**, *44*, 1456−1477.

10.1021/jo051430g CCC: $30.25
Published on Web 10/18/2005

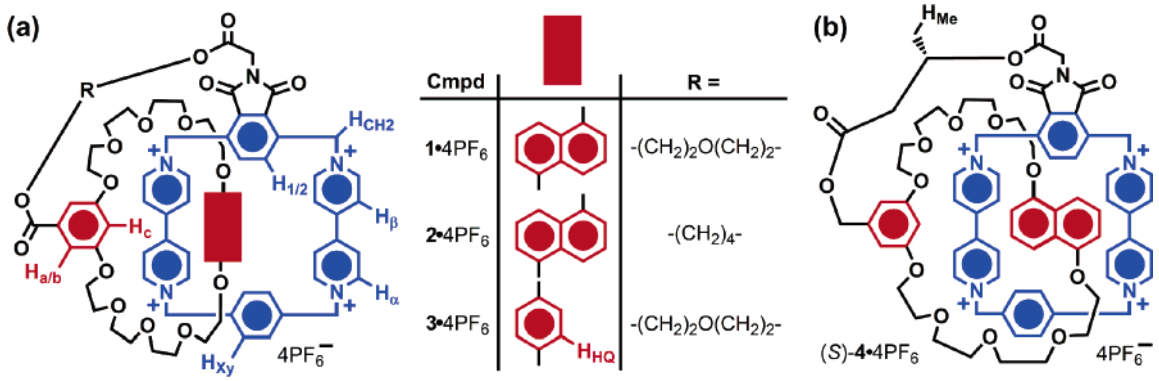

FIGURE 2. Structural formulas for the donor–acceptor pretzelanes (a) **1**·4PF_6–**3**·4PF_6 and (b) (*S*)-**4**·4PF_6.

stitutions of the ring components. While it may be tempting to describe these systems as topologically chiral, in fact they are not. Indeed, the concept of "residual topological isomerism" has been introduced[12] to describe this pseudotopological chirality.

In more recent times, we have been investigating[13] some donor–acceptor pretzelanes (Figure 2). These compounds are composed of an electron-deficient tetracationic cyclophane connected via a tether to, and mechanically interlocked with, an electron-rich macrocyclic polyether. It was shown that, by varying the length of the tether, the major product could be directed toward either a cyclic bis[2]catenane or a pretzelane architecture. The X-ray crystal structure (Figure 3) of the pretzelane **1**·4PF_6 indicates[13] the presence of [$\pi\cdots\pi$],[14] [C–H···O],[15] and [C–H···π][16] interactions between the cyclophane and the macrocycle in these compounds. Additionally, the coconformations adopted by these donor–acceptor pretzelanes give rise to the possibility for multiple diastereoisomers that can be dynamically exchanged in a manner reminiscent of the related[17] donor–acceptor [2]catenanes.

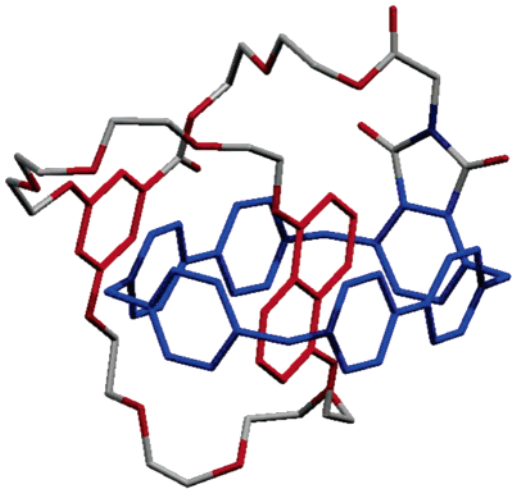

FIGURE 3. The X-ray crystal structure of pretzelane **1**·4PF_6.

The classical (Euclidean) chirality present in these pretzelanes has been probed by using chiral anions[13] and introducing[18] a chiral center into the tether. Here, we will discuss the dynamic stereochemistry of the donor–acceptor pretzelanes in more detail and investigate the

(6) (a) Chichak, K. S.; Cantrill, S. J.; Pease, A. R.; Chiu, S.-H.; Cave, G. W. V.; Atwood, J. L.; Stoddart, J. F. *Science* **2004**, *304*, 1308–1312. (b) Siegel, J. S. *Science* **2004**, *304*, 1256–1258. (c) Schalley, C. A. *Angew. Chem., Int. Ed.* **2004**, *43*, 4399–4401. (d) Chichak, K. S.; Cantrill, S. J.; Stoddart, J. F. *Acc. Chem. Res.* **2005**, *38*, 1-9. (e) Chichak, K. S.; Cantrill. S. J.; Stoddart, J. F. *Chem. Commun.* **2005**, 3391–3393. (f) Peters, A. J.; Chichak, K. S.; Cantrill, S. J.; Stoddart, J. F. *Chem. Commun.* **2005**, 3394–3396.

(7) (a) Tseng, H.-R.; Wu, D.; Fang, N. X.; Zhang, X.; Stoddart, J. F. *ChemPhysChem* **2004**, *5*, 111–116. (b) Kang, S.; Vignon, S. A.; Tseng, H.-R.; Stoddart, J. F. *Chem. Eur. J.* **2004**, *10*, 2555–2564. (c) Steuerman, D. W.; Tseng, H.-R.; Peters, A. J.; Flood, A. H.; Jeppesen, J. O.; Nielsen, K. A.; Stoddart, J. F.; Heath, J. R. *Angew. Chem., Int. Ed.* **2004**, *43*, 6486-6491. (d) Flood, A. H.; Peters, A. J.; Vignon, S. A.; Steuerman, D. W.; Tseng, H.-R.; Kang, S.; Heath, J. R.; Stoddart, J. F. *Chem. Eur. J.* **2004**, *10*, 6558–6564. (e) Vignon, S. A.; Stoddart, J. F. *Collect. Czech. Chem. Commun.* **2005**, in press.

(8) (a) Balzani, V.; Credi, A.; Raymo, F. M.; Stoddart, J. F. *Angew. Chem., Int. Ed.* **2000**, *112*, 3484–3530. (b) Balzani, V.; Credi, A.; Venturi, M. *Molecular Devices and Machines—A Journey into the Nano World*; Wiley-VCH: Weinheim, Germany, 2003; (c) Flood, A. H.; Ramirez, R. J. A.; Deng, W.-Q.; Muller, R. P.; Goddard, W. A., III; Stoddart, J. F. *Aust. J. Chem.* **2004**, *57*, 301–322.

(9) (a) Collier, C. P.; Mattersteig, G.; Wong, E. W.; Luo, Y.; Beverly, K.; Sampaio, J.; Raymo, F. M.; Stoddart, J. F.; Heath, J. R. *Science* **2000**, *289*, 1172–1175. (b) Pease, A. R.; Jeppesen, J. O.; Stoddart, J. F.; Luo, Y.; Collier, C. P.; Heath, J. R. *Acc. Chem. Res.* **2001**, *34*, 433–444. (c) Luo, Y.; Collier, C. P.; Jeppesen, J. O.; Nielsen, K. A.; DeIonno, E.; Ho, G.; Perkins, J.; Tseng, H.-R.; Yamamoto, T.; Stoddart, J. F.; Heath, J. R. *ChemPhysChem* **2002**, *3*, 519–525. (d) Diehl, M. R.; Steuerman, D. W.; Tseng, H.-R.; Vignon, S. A.; Star, A.; Celestre, P. C.; Stoddart, J. F.; Heath, J. R. *ChemPhysChem* **2003**, *4*, 1335–1339. (e) Flood, A. H.; Stoddart, J. F.; Steuerman, D. W.; Heath, J. R. *Science* **2004**, *306*, 2055–2056. (f) Mendes, P. M.; Flood, A. H.; Stoddart, J. F. *Appl. Phys. A* **2005**, *80*, 1197–1209.

(10) (a) Jäger, R.; Schmidt, T.; Karbach, D.; Vögtle, F. *Synlett* **1996**, 723–725. (b) Mohry, A.; Schwierz, H.; Vögtle, F. *Synthesis* **1999**, *10*, 1753–1758. (c) Li, Q. Y.; Vogel, E.; Parham, A. H.; Nieger, M.; Bolte, M.; Fröhlich, R.; Saarenketo, P.; Rissanen, K.; Vögtle, F. *Eur. J. Org. Chem.* **2001**, 4041–4049.

(11) (a) Yamamoto, C.; Okamoto, Y.; Schmidt, T.; Jäger, R.; Vögtle, F. *J. Am. Chem. Soc.* **1997**, *119*, 10547–10548. (b) Vögtle, F.; Safarowsky, O.; Heim, C.; Affeld, A.; Braun, O.; Mohry, A. *Pure Appl. Chem.* **1999**, *71*, 247–251. (c) Reuter, C.; Mohry, A.; Sobanski, A.; Vögtle, F. *Chem. Eur. J.* **2000**, *6*, 1674–1682.

(12) Lukin, O.; Godt, A.; Vögtle, F. *Chem. Eur. J.* **2004**, *10*, 1878–1883.

(13) Liu, Y.; Bonvallet, P. A.; Vignon, S. A.; Khan, S. I.; Stoddart, J. F. *Angew. Chem., Int. Ed.* **2005**, *44*, 3050–3055.

(14) Hunter, C. A.; Sanders, J. K. M. *J. Am. Chem. Soc.* **1990**, *112*, 5525–5534.

(15) (a) Desiraju, G. R. *Acc. Chem. Res.* **1996**, *29*, 441–449. (b) Houk, K. N.; Menzer, S.; Newton, S. P.; Raymo, F. M.; Stoddart, J. F.; Williams, D. J. *J. Am. Chem. Soc.* **1999**, *121*, 1479–1487. (c) Raymo, F. M.; Bartberger, M. D.; Houk, K. N.; Stoddart, J. F. *J. Am. Chem. Soc.* **2001**, *123*, 9264–9267.

(16) Nishio, M.; Umezawa, Y.; Hirota, M.; Takeuchi, Y. *The C–H···π Interaction*; Wiley-VCH: New York, 1998.

(17) Tseng, H.-R.; Vignon, S. A.; Celestre, P. C.; Stoddart, J. F.; White, A. J. P.; Williams, D. J. *Chem. Eur. J.* **2003**, *9*, 543–556.

(18) Liu, Y.; Vignon, S. A.; Zhang, X.; Houk, K. N.; Stoddart, J. F. *Chem. Commun.* **2005**, 3927–3929.

SCHEME 1. Synthesis of Pretzelanes 1·4PF$_6$ and 2·4PF$_6$[a]

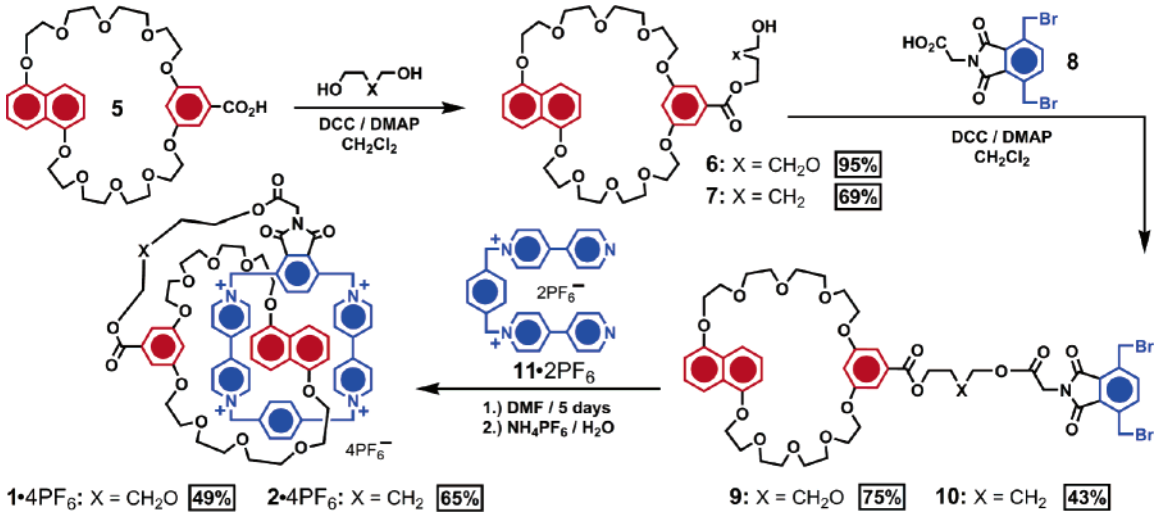

[a] DCC = *N,N*′-dicyclohexylcarbodiimide, DMAP = *N,N*-dimethyl-4-aminopyridine, DMF = *N,N*-dimethylformamide.

effects of changing their constitution and introducing fixed chirality.

Results and Discussion

Synthesis. To explore the effects of the tether and other structural features on the dynamic and stereochemical properties of these compounds, several different pretzelanes have been designed and synthesized. The syntheses of the DNP-containing pretzelanes **1**·4PF$_6$[13] and **2**·4PF$_6$ are outlined in Scheme 1. Reaction of **5**[19] carrying a symmetrically positioned carboxyl group with an excess of diethylene glycol or 1,4-butandiol gave the corresponding alcohol **6** or **7**, respectively, which then underwent esterification with another carboxylic acid derivative **8**[20] to afford a key intermediate, either dibromide **9** or **10**. Formation of **1**·4PF$_6$ and **2**·4PF$_6$ was achieved in yields of 49% and 65%, respectively, by allowing either **9** or **10** and **11**·2PF$_6$[21] to be stirred in DMF (*N,N*-dimethylformamide) for 5 days before exchanging counterions.

The hydroquinone-containing pretzelane **3**·4PF$_6$ was synthesized (Scheme 2) following a procedure similar to that used for the syntheses of **1**·4PF$_6$ and **2**·4PF$_6$. The crown ether **12** (Scheme 2) was prepared according to literature procedures.[22] Subsequently, esterification of **12** by reaction with an excess of diethylene glycol gave **13** in 69% yield. Another esterification followed to couple the dibromide **8** with the alcohol **13** in 35% yield after purification. A solution of the substituted crown ether **14** was then mixed with **11**·2PF$_6$ in DMF for 5 days to allow the template-directed clipping reaction to occur. After purification by column chromatography and counterion exchange, the pretzelane **3**·4PF$_6$ was obtained in 25% yield as an orange solid.

Finally, the chiral pretzelane (*S*)-**4**·4PF$_6$ was synthesized[18] in a similar fashion (Scheme 3). Reaction of **15** carrying a symmetrically positioned hydroxyl group with the carboxylic acid (*S*)-**16**[23] gave the compound (*S*)-**17**. Removal of the TBDMS protecting group generated the alcohol (*S*)-**18**, which underwent esterification with the carboxylic acid derivative **8** to afford the key intermediate, the dibromide (*S*)-**19**. Formation of (*S*)-**4**·4PF$_6$ was achieved in 27% yield by allowing (*S*)-**19** and **11**·2PF$_6$ to stir in DMF for 3 days at 14 kbar and then exchanging the counterions.

SCHEME 2. Synthesis of Pretzelane 3·4PF$_6$

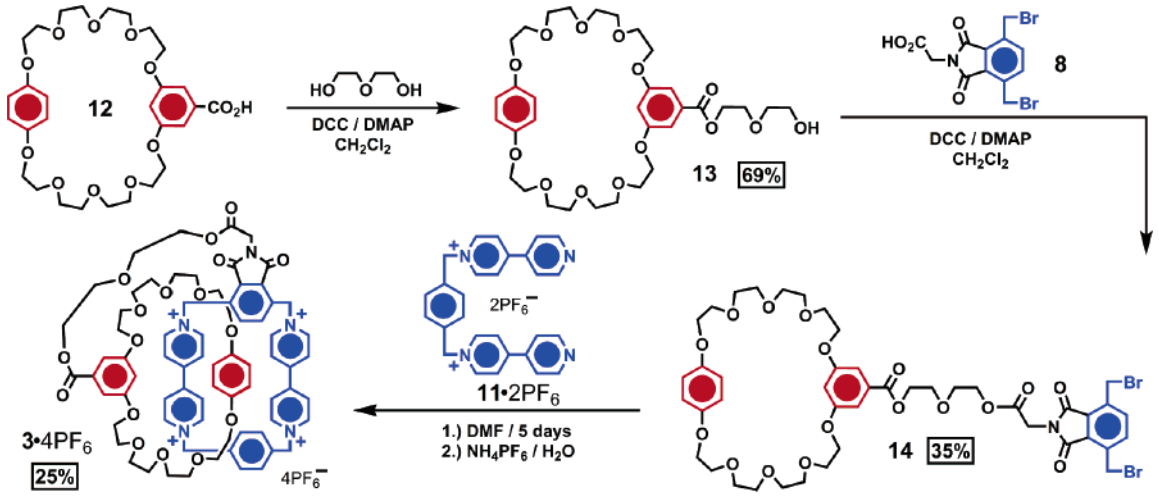

SCHEME 3. Synthesis of the Chiral Pretzelane (*S*)-4·4PF$_6$

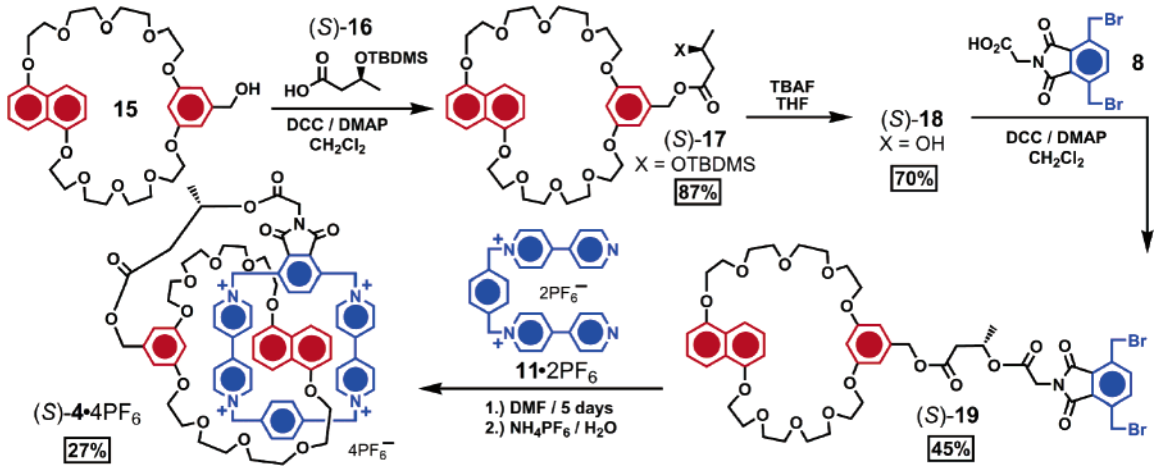

Stereochemistry. Several elements of chirality (Figure 4) are present in these compounds and are responsible for the multitude of possible diastereoisomers. All of these chiral elements are classical (Euclidean) in nature, i.e., nontopological chirality that arises from the geometry of the conformations adopted and can be inverted by unrestricted deformation of the structure without forming or breaking any bonds. For example, if a 1,5-dioxynaphthalene (DNP) unit is present in the pretzelane, then an element of planar chirality[24] is present (Figure 4a) that depends on the orientation of the DNP with respect to the macrocycle containing it. This chirality is indicated as either (*pR*) or (*pS*).

The other two elements of chirality arise from the relative orientation of the two ring components of the pretzelane with respect to one another. The first results (Figure 4b) from the loss of symmetry in the tetracationic cyclophane through fusion of a diimide anchor. The two bipyridinium units are now enantiotopic, and hence the two conformations (Figure 4b) become enantiomers. Rules for describing this element of chirality have been described[13] previously, and we have chosen to use the descriptors (*P*) and (*M*) to describe it.

The last chiral element is also a result (Figure 4c) of the relative orientation of the two ring components—in this case the ~45° angle of the mean planes of the rings with respect to one another. This so-called helical chirality has been investigated[17] extensively in related donor–acceptor [2]catenanes, including its observation[25] by ^{1}H NMR spectroscopy with use of chiral shift reagents. The rules for describing this chirality have also been presented[17] previously. Briefly, the higher priority ring is oriented in front and an arrow drawn from the high priority ring to the lower priority one via the shortest path determines if the chirality is (*P*), clockwise arrow, or (*M*), counterclockwise arrow. This chirality interacts intimately with the planar chirality of a DNP unit if present in these donor–acceptor systems: thus, in cases where both chiral elements are present in the same compound, the configuration of one is often determined by that of the other.

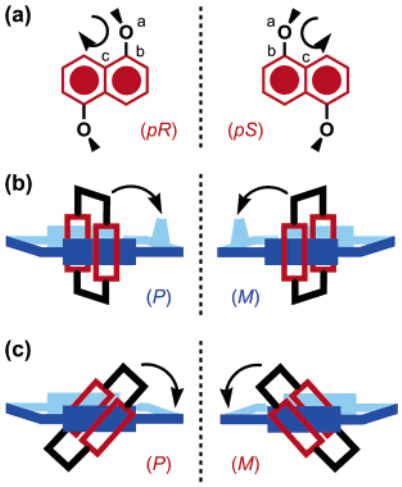

FIGURE 4. Schematic representations of the stereoelements present in donor–acceptor pretzelanes. Specifically, (a) planar chirality arising from the DNP unit, (b) helical chirality arising from orientation of the crown ether macrocycle relative to the diimide moiety, and (c) helical chirality arising from the relative orientation of the two rings. See text for details on nomenclature.

An interesting aspect of these chiral elements present in donor–acceptor pretzelanes is their dynamic nature. All three can be inverted by one or more dynamic

(19) Menzer, S.; White, A. J. P.; Williams, D. J.; Belohradsky, M.; Hamers, C.; Raymo, F. M.; Shipway, A. N.; Stoddart, J. F. *Macromolecules* **1998**, *31*, 295–307.
(20) (a) Liu, Y.; Flood, A. H.; Stoddart, J. F. *J. Am. Chem. Soc.* **2004**, *126*, 9150–9151. (b) Liu, Y.; Flood, A. H.; Moskowitz, R. M.; Stoddart, J. F. *Chem. Eur. J.* **2005**, *11*, 369–385.
(21) Ashton, P. R.; Goodnow, T. T.; Kaifer, A. E.; Reddington, M. V.; Slawin, A. M. Z.; Spencer, N; Stoddart, J. F.; Vicent, C.; Williams, D. J. *Angew. Chem., Int. Ed. Engl.* **1989**, *28*, 1396–1399.
(22) Gibson, H. W.; Nagvekar, D. S.; Yamaguchi, N.; Wang, F.; Bryant, W. S. *J. Org. Chem.* **1997**, *62*, 4798–4803.
(23) Kobayashi, Y.; Kumar, G. B.; Kurachi, T.; Acharya, H. P.; Yamazaki, T.; Kitazume, T. *J. Org. Chem.* **2001**, *66*, 2011–2018.
(24) Eliel, E. L.; Wilen, S. H. *Stereochemistry of Organic Compounds*; Wiley: New York, 1994; Chapter 14.
(25) Vignon, S. A.; Wong, J.; Tseng, H.-R.; Stoddart, J. F. *Org. Lett.* **2004**, *6*, 1095–1098.
(26) (a) Asakawa, M.; Ashton, P. R.; Boyd, S. E.; Brown, C. L.; Gillard, R. E.; Kocian, O.; Raymo, F. M.; Stoddart, J. F.; Tolley, M. S.; White, A. J. P.; Williams, D. J. *J. Org. Chem.* **1997**, *62*, 26–37. (b) Bravo, J. A.; Raymo, F. M.; Stoddart, J. F.; White, A. J. P.; Williams, D. J. *Eur. J. Org. Chem.* **1998**, 2565–2571. (c) Cabezon, B.; Cao, J.; Raymo, F. M.; Stoddart, J. F.; White, A. J. P.; Williams, D. J. *Chem. Eur. J.* **2000**, *6*, 2262–2273.

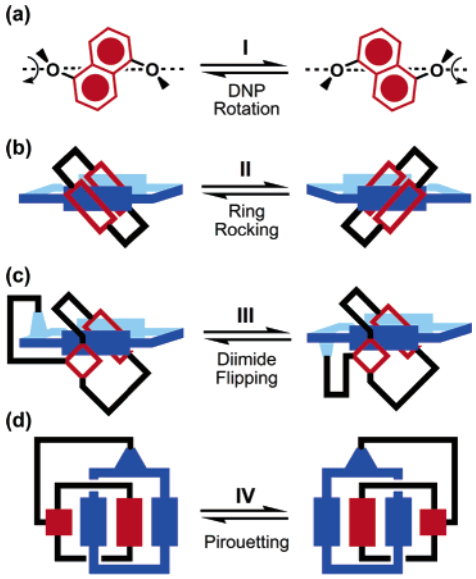

FIGURE 5. Schematic representations of the dynamic processes occurring in donor−acceptor pretzelanes. Specifically, (a) rotation of the DNP unit about its substitution axis, (b) rocking of one ring with respect to the other one, (c) rotation of the benzodiimide unit about its substitution axis, and (d) pirouetting of the crown ether macrocycle about the tetracationic cyclophane.

processes that occur with barriers ranging from 10 to 20 kcal mol^{-1}. Process I, DNP rotation[26] (Figure 5a), involves rotation of the DNP unit about its substitution axis leading to inversion of the planar chirality (Figure 4a) associated with this unit. Similarly, ring rocking (Process II in Figure 5b) inverts the helical chirality (Figure 4c) associated with tilting of the two ring components. This process represents a rotation about the mechanical bond of ~90° of one ring component relative to the other.

The third process (Process III in Figure 5c) has been dubbed diimide flipping because it involves rotation of the benzodiimide unit about its substitution axis. The net result of this process is to invert the helical chirality associated with the orientation of the crown ether macrocycle relative to that of the diimide moiety (Figure 4b). The final process to be discussed here (Process IV in Figure 5d) involves pirouetting of the crown ether macrocycle about the tetracationic cyclophane. As a result of this process, all three chiral elements (Figure 4a−c) are inverted. The combination of these three chiral elements and four dynamic processes leads to each donor−acceptor pretzelane existing as a dynamic combinatorial library of diastereoisomers. In the next section, the results of a ^{1}H NMR spectroscopic investigation of these compounds will be presented.

NMR Spectroscopy. A variable-temperature ^{1}H NMR spectroscopic study was performed on all four pretzelanes to determine the nature of their dynamic processes occurring in solution. The ^{1}H NMR spectrum (Figure 6b) of **1**·4PF$_6$, reveals that, at low temperature where the dynamic processes are slow on the ^{1}H NMR time scale, all of the protons in the molecule become heterotopic. Upon increasing the temperature and recording the spectrum (Figure 6a) again, many of the signals are observed to coalesce[27] into averaged signals as a result of the increasing rate of exchange. Several different processes are responsible for exchanging the different protons, and in some cases multiple processes can exchange the same pairs of protons. To fully understand the dynamic processes in these donor−acceptor pretzelanes, the diastereoisomers being exchanged must also be considered.

A schematic diagram for exchange in **1**·4PF$_6$ is shown in Figure 7. We have previously determined[13] that the (*pR*)-(*M*)-(*P*)/(*pS*)-(*P*)-(*M*) enantiomeric pair of diastereoisomers is the lowest energy configuration for **1**·4PF$_6$. If any of the other diastereoisomers are present in solution, then the amount is too small to be detected by ^{1}H NMR spectroscopy. For degenerate exchange to occur in this pretzelane, two pathways are possible: either (i) direct inversion of all the chiral elements via pirouetting (Process IV) or (ii) a combination of processes (Processes I, II, and III), with the higher energy diastereoisomer (*pR*)-(*M*)-(*M*)/(*pS*)-(*P*)-(*P*) serving as an intermediate. To

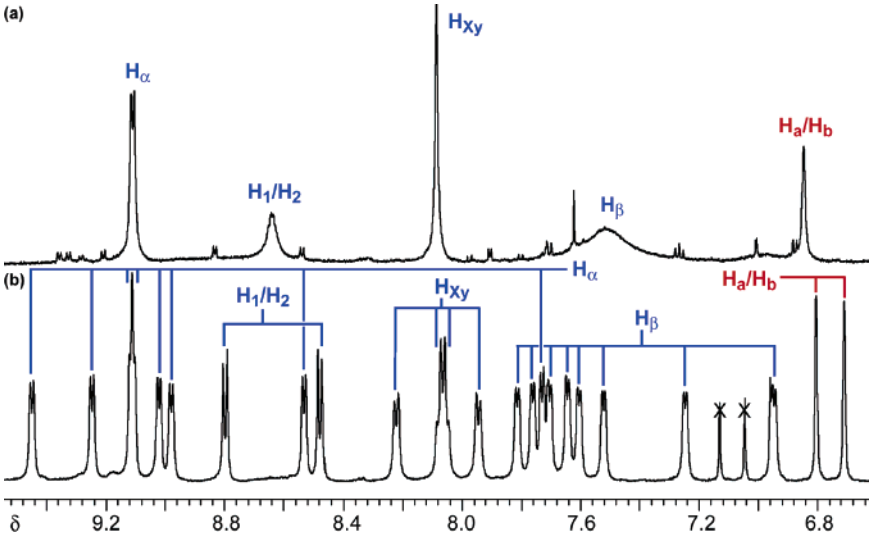

FIGURE 6. The 600 MHz ^{1}H NMR spectra for **1**·4PF$_6$ recorded in CD_3SOCD_3 at (a) 378 and (b) 301 K. See Figure 2 for structural assignments.

determine the relative preference for these two pathways, it was necessary to identify pairs of protons that are only exchanged by one pathway or the other. Careful examination of the structure of **1**·4PF$_6$ revealed that the benzodiimide protons (H$_1$/H$_2$) are exchanged in degenerate fashion only via Process IV, while the protons H$_a$/H$_b$ are exchanged degenerately only by the combination of Processes I, II, and III. Spin saturation transfer (SST) experiments[28] were then performed on these two sets of protons to determine the rates of exchange (k_{ex}).

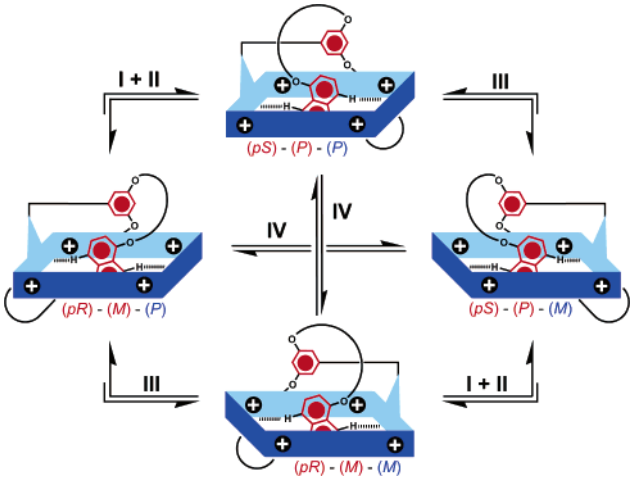

FIGURE 7. Schematic representations of some possible diastereoisomers for **1**·4PF$_6$ and **2**·4PF$_6$ and their exchange pathways. Not all possible diastereoisomers are shown. See text for details.

The data for **1**·4PF$_6$ in CD_3SOCD_3 and CD_3CN are summarized in Table 1. An initial examination of these data reveals that the barriers for the two pathways are the same within experimental error. This observation suggests that the two pathways share a common intermediate, which is likely to involve removing the DNP unit from the cavity of the tetracationic cyclophane. Indeed, examination of molecular models suggests that this step is a necessary one for both pirouetting and DNP rotation. The disruption of some of the intramolecular interactions in CD_3SOCD_3 is also apparent in the ~0.4 kcal mol^{-1} lower barrier for both pathways in this solvent relative to CD_3CN.

TABLE 1. Kinetic and Thermodynamic Data for 1·4PF$_6$

solvent	process	T[a]	k_{ex}[b]	$\Delta G^{\ddagger}$[c]
CD_3SOCD_3	IV[d]	294	0.4	17.7
		301	1.0	17.6
	I + II + III[e]	294	0.5	17.6
		301	1.2	17.5
CD_3CN	IV[d]	306	1.0	18.0
		317	1.9	18.2
	I + II + III[e]	294	0.3	18.0
		306	1.0	18.0
		317	1.9	18.2

[a] K, calibrated with neat MeOH. [b] s^{-1}, measured with spin saturation transfer (ref 28). [c] kcal mol^{-1}, ±0.1. [d] Exchange observed between H$_1$/H$_2$. [e] H$_a$/H$_b$. See Figure 2 for structural assignments.

To examine the effects of structural changes on the barriers associated with these two pathways, the pretzelane **2**·4PF$_6$, where the tether is shorter and more hydrophobic than in **1**·4PF$_6$, was investigated. The ^{1}H NMR spectrum (Figure 8b) of **2**·4PF$_6$ in CD_3SOCD_3 recorded at low temperature is very similar to that observed (Figure 6b) for **1**·4PF$_6$, with no evidence for the presence of more than one diastereoisomer. The major diastereoisomer in **2**·4PF$_6$ was assumed to be the same one as in **1**·4PF$_6$ because of their structural similarity. Upon increasing the temperature, many of the signals are observed (Figure 8a) to coalesce, and so SST experiments were performed to obtain data on the exchange processes. As in the case of **1**·4PF$_6$, the data for **2**·4PF$_6$ show (Table 2) identical barriers for the two pathways, again suggesting similar mechanisms. A comparison of

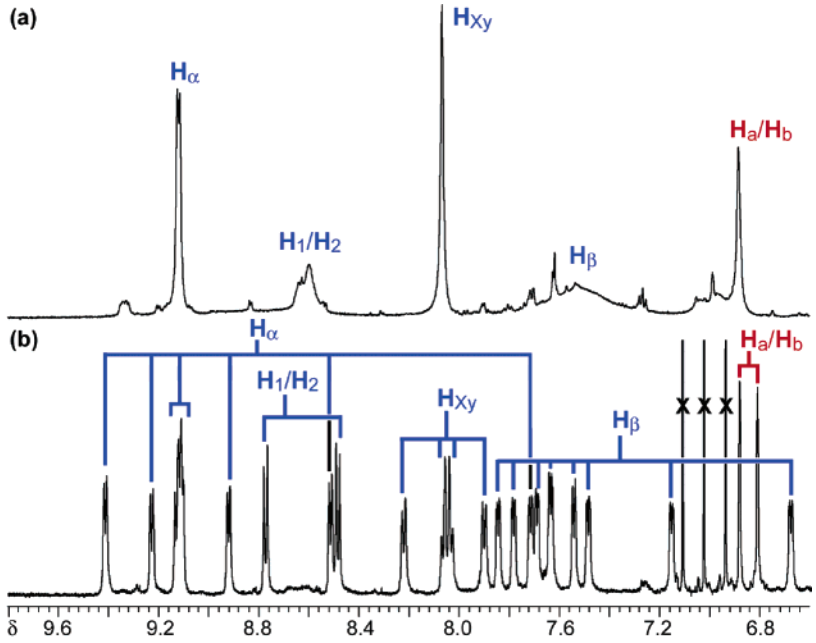

FIGURE 8. The 600 MHz ^{1}H NMR spectra for **2**·4PF$_6$ recorded in CD_3SOCD_3 at (a) 375 and (b) 311 K. See Figure 2 for structural assignments.

TABLE 2. Kinetic and Thermodynamic Data for 3·4PF$_6$

solvent	process	T^a	$k_{ex}{}^b$	$\Delta G^{\ddagger}{}^c$
CD_3SOCD_3	IV[d]	294	0.3	17.9
		300	0.6	17.8
	I + II + III[e]	294	0.3	17.9
		300	0.6	17.8
CD_3CN	IV[d]	300	0.2	18.6
		307	0.4	18.5
	I + II + III[e]	294	0.1	18.8
		300	0.2	18.6
		307	0.4	18.6

[a] K, calibrated with neat MeOH. [b] s^{-1}, measured with spin saturation transfer (ref 28). [c] kcal mol^{-1}, ±0.1. [d] Exchange observed between H_1/H_2. [e] H_a/H_b. See Figure 2 for structural assignments.

the data obtained in CD_3CN for these two pretzelanes, however, reveals a larger barrier by ~0.5 kcal mol^{-1} for **2**·4PF$_6$, with a slightly smaller difference (~0.2 kcal mol^{-1}) in CD_3SOCD_3, relative to **1**·4PF$_6$. Thus, it appears that the shorter tether poses a greater challenge for the dynamic processes observed in **2**·4PF$_6$, but does not change the identity of their common intermediate.

The pretzelane **3**·4PF$_6$, which contains a hydroquinone (HQ) unit, was subsequently investigated to determine if the equivalence of the two pathways is dependent on the presence of a DNP unit and its associated planar chirality. The exchange pathways (Figure 9) for **3**·4PF$_6$ are similar to those for the two DNP-containing pretzelanes, with the exception that the pathway passing through the less favorable diastereoisomer no longer requires DNP rotation (Process I). The low-temperature ^{1}H NMR spectrum (Figure 10b) of **3**·4PF$_6$ in CD_3CN shows that all the protons are heterotopic and that the compound exists as a single enantiomeric pair of diastereoisomers within the limits of detection by ^{1}H NMR spectroscopy. This diastereoisomer was assigned as the (*M*)-(*P*) one based on previous observations in **1**·4PF$_6$. Recording the ^{1}H NMR spectrum again at high temperature reveals the onset of coalescence (Figure 10a). As with the DNP-containing pretzelanes, the two exchange pathways could be investigated by observing the exchange of H_1/H_2 and H_a/H_b, using SST experiments, and in this case, also by partial line shape analysis.[29] The resulting data for **3**·4PF$_6$ are presented in Table 3.

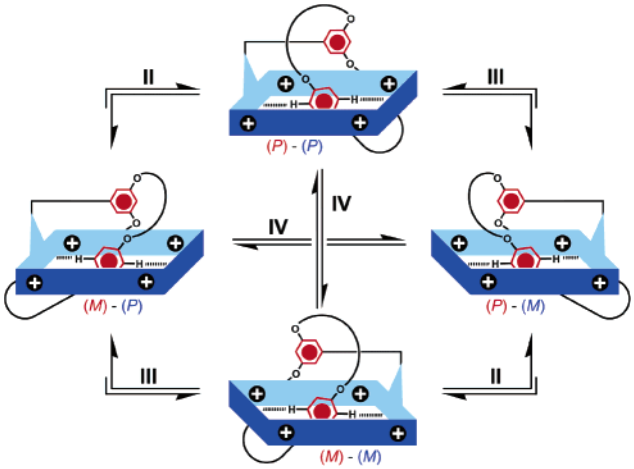

FIGURE 9. Schematic representation of the possible diastereoisomers for **3**·4PF$_6$ and their exchange pathways.

A quick perusal of these data reveals that the barriers for this HQ-containing pretzelane are significantly lower than those for the DNP-containing ones. Pirouetting in CD_3CN, for example, is ~2−3 kcal mol^{-1} lower in **3**·4PF$_6$ than in **1**·4PF$_6$ or **2**·4PF$_6$. Perhaps more importantly, however, the two pathways possess significantly different barriers in this case. Pirouetting (Process IV) has the larger barrier, with a value of 16.4 kcal mol^{-1} at 317 K in CD_3CN, while the barrier for the alternative pathway (Processes II and III) can be associated with a barrier of 14.5 kcal mol^{-1} under the same conditions. These observations suggest that these two pathways no

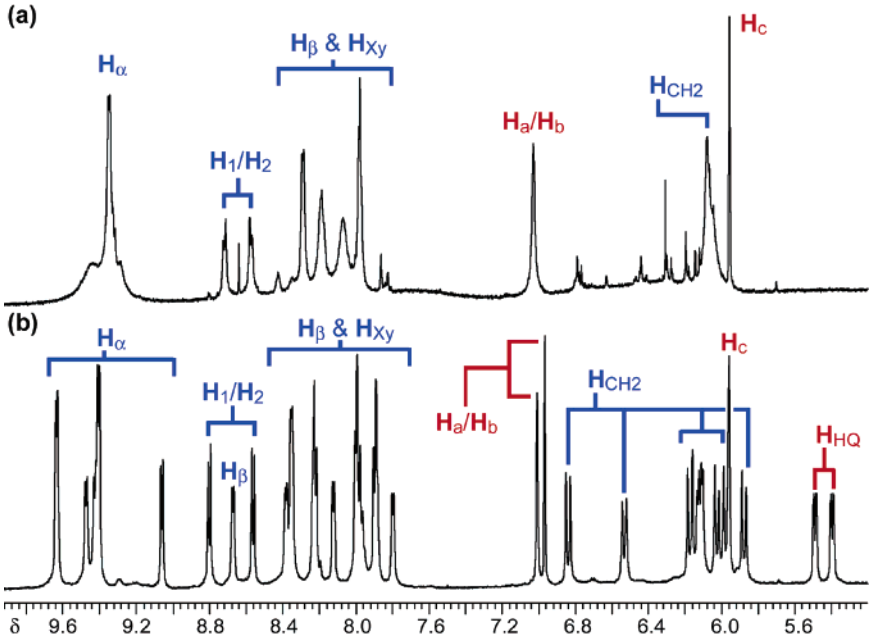

FIGURE 10. The 600 MHz ^{1}H NMR spectra for **3**·4PF$_6$ recorded in CD_3COCD_3 at (a) 311 and (b) 205 K. See Figure 2 for structural assignments.

TABLE 3. Kinetic and Thermodynamic Data for 3·4PF$_6$

solvent	process	T^a	k_{ex}	$\Delta G^{\ddagger}$ [b]
CD_3COCD_3	IV [e]	275	0.4[c]	16.6
		293	1.9[c]	16.8
	II + III[f]			
CD_3CN	IV[e]	293	7[d]	16.0
		317	35[d]	16.4
		332	110[d]	16.4
	II + III[f]	225	0.5[c]	13.4
		247	3[d]	13.8
		277	35[d]	14.2
		317	650[d]	14.5

[a] K, calibrated using neat MeOH. [b] kcal mol^{-1}, ±0.1. [c] s^{-1}. measured using spin saturation transfer (ref 28). [d] s^{-1}, measured using partial line shape analysis. [e] Exchange observed between H_1/H_2. See Figure 2 for structural assignments. [f] Exchange observed between H_a/H_b. See Figure 2 for structural assignments.

longer share a common intermediate in **3**·4PF$_6$, a suggestion that can be rationalized by realizing that the HQ unit must be removed from the cavity for pirouetting to occur, but the same requirement does not exist for Process I or II. Thus, the multistep pathway has a lower barrier as a consequence of the decreased disruption of intramolecular interactions, specifically the [$\pi\cdots\pi$] interactions between the HQ unit and the tetracationic cyclophane.

To determine if the helical chirality associated with the diimide moiety (Figure 4b) can be influenced, a fixed element of chirality was inserted into the tether of a DNP-containing pretzelane. The resulting compound, (*S*)-**4**·4PF$_6$, can exchange (Figure 11) between two diastereoisomers, namely, (*S*)-(*pR*)-(*M*)-(*P*) and (*S*)-(*pS*)-(*P*)-(*M*), via either of the two pathways investigated in the achiral pretzelanes. The ^{1}H NMR spectrum of this compound was recorded (Figure 12) at low temperature in CD_3SOCD_3 and revealed two sets of unequal intensity signals corresponding to the two diastereoisomers. Integration of the signals for the H_{Me} proton in CD_3SOCD_3 (δ 1.45 and 1.54 ppm) and CD_3CN (δ 1.44 and 1.53 ppm) gave ratios of 6:1 and 9:1, respectively. From these values the free energy difference for the two diastereoisomers can be calculated to be $\Delta G° = 1.3$ kcal mol^{-1} in CD_3CN at 298 K.

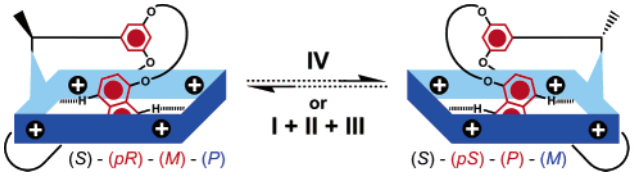

FIGURE 11. Schematic representation of two of the possible diastereoisomers for the chiral pretzelane (*S*)-**4**·4PF$_6$ and the possible exchange processes.

The structures of these diastereoisomers were investigated[18] by force-field modeling. Input geometries for the two diastereoisomers, (*S*)-(*pR*)-(*M*)-(*P*) and (*S*)-(*pS*)-(*P*)-(*M*), were created by using the X-ray crystal structure of **1**·4PF$_6$ and modifying it accordingly. Several different force fields gave values ranging from 2.3 to 6.3 kcal mol^{-1} for the energy difference between the two diastereoisomers: in all cases, however, the (*S*)-(*pS*)-(*P*)-(*M*) isomer was predicted to be more favorable. The resulting structures (Figure 13) show clearly why one is preferred over the other. The conformation (Figure 13a) of (*S*)-(*pR*)-(*M*)-(*P*) has the methyl group attached to the chiral center of the tether pointing inward toward the crowded cavity of the tetracationic cyclophane. On the other hand, the (*S*)-(*pS*)-(*P*)-(*M*) isomer exists in a conformation (Figure 13b) where this methyl group is pointing outward. In both cases, all of the expected noncovalent interactions remain intact, suggesting that the preference arises primarily from this steric effect. It is also interesting to note that the chemical shifts of the protons for this methyl group, H_{Me}, support the calculated structures. In other words, the chemical shift of H_{Me} in the less preferred isomer (δ = 1.54 ppm) is shifted further downfield because of its proximity (Figure 13a) to the aromatic DNP unit, while the major conformation places the methyl group farther away (Figure 13a) from this source of diamagnetic shielding, leading to an upfield shift (δ = 1.45 ppm).

To understand how the two diastereoisomers exchange, SST experiments were performed by observing the H_{Me} signals in a sample of (*S*)-**4**·4PF$_6$ in CD_3SOCD_3. The data for this exchange process are presented in Table 4. The barrier ($\Delta G^{\ddagger}$) to diastereoisomeric exchange in this chiral pretzelane of 17.8 kcal mol^{-1} at 301 K in CD_3SOCD_3 is very similar to those observed (Tables 1 and 2) for the achiral DNP-containing pretzelanes under similar conditions. This observation suggests that the dynamic ex-

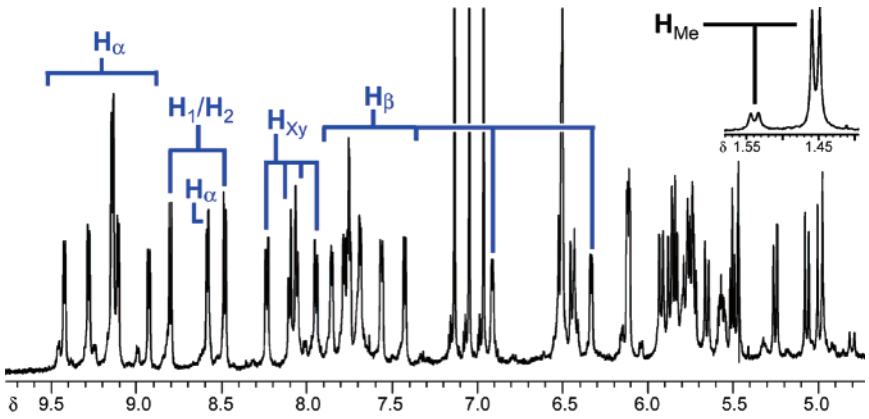

FIGURE 12. The 600 MHz ^{1}H NMR spectrum for the chiral pretzelane (*S*)-**4**·4PF$_6$ recorded in CD_3SOCD_3 at 290 K. See Figure 2 for structural assignments.

TABLE 4. Kinetic and Thermodynamic Data for (*S*)-4·4PF$_6$

solvent	protons	T^a	$k_{ex}{}^b$	$\Delta G^{\ddagger}{}^c$
CD_3SOCD_3	H_{Me}	301	0.8	17.8
		313	2.3	17.8

[a] K, calibrated with neat MeOH. [b] s^{-1}, measured with spin saturation transfer (ref 28). The H_{Me} proton at 1.54 ppm was irradiated and the signal at 1.45 ppm was observed. [c] kcal mol^{-1}, ±0.1.

change mechanism remains the same, except it is no longer a degenerate one in the case of (*S*)-**4**·4PF$_6$.

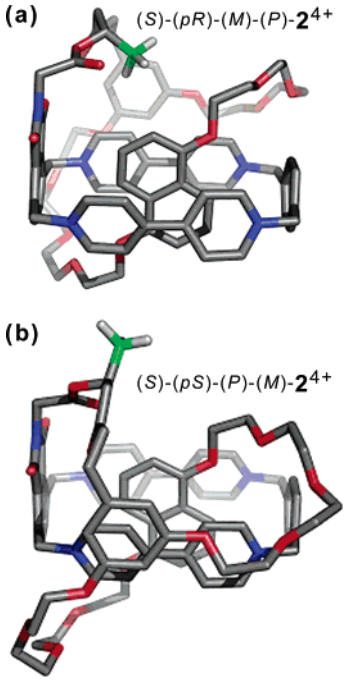

FIGURE 13. The calculated structures (MM2 force field) for the two diastereoisomers of (*S*)-**4**·4PF$_6$.

CD Spectroscopy. CD spectra were also recorded (Figure 14) for (*S*)-**4**·4PF$_6$ in MeCN over a range of temperatures. Two responses were observed in these spectra at λ_{max} = 340 and 506 nm. These signals correspond to the bipyridinium absorption and the charge transfer band between the DNP unit and the bipyridinium units, respectively. These observations suggest that the fixed element of chirality inserted into the tether induces chirality in other parts of the pretzelane, namely in the region involved in donor−acceptor interactions. A moderate temperature dependence was also observed, where the intensities of the CD bands are observed to decrease with increasing temperature. While it is unclear what is responsible for this trend, it could be a result of

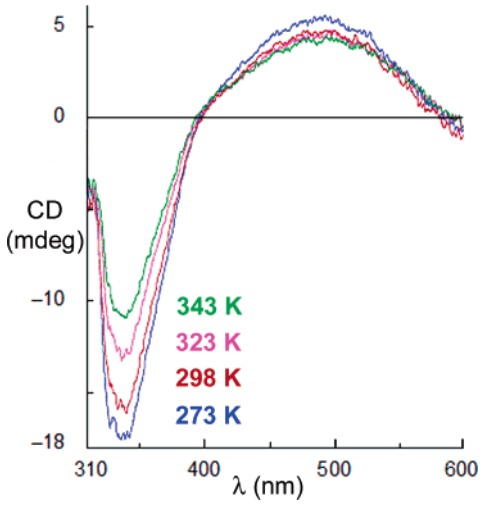

FIGURE 14. CD spectra recorded in MeCN at different temperatures of the chiral pretzelane (*S*)-**4**·4PF$_6$.

a change in the equilibrium between the (*S*)-(*pR*)-(*M*)-(*P*) and (*S*)-(*pS*)-(*P*)-(*M*) diastereoisomers.

Conclusions

Here, we have described the ability to influence both the rate and mechanism of the dynamic stereochemistry inherent to a small group of donor−acceptor pretzelanes as a result of structural modifications. These pretzelanes exist as dynamic libraries of stereoisomers reminiscent of those observed in related donor−acceptor [2]catenanes, and, as in the case of catenanes, only a single enantiomeric pair of diastereoisomers dominates in solution. By inserting an element of fixed chirality into the tether component, it was possible to perturb the balance and create a situation where two diastereoisomers can be observed. The observation that these diastereoisomers in the chiral pretzelane continue to exchange, with what appears to be the same rate and mechanism as the achiral ones, bodes well for future efforts to control the dynamic stereochemistry of these systems.

Of particular interest is the similarity of the kinetic and thermodynamic parameters observed here for donor−acceptor pretzelanes to those observed[7] in donor−acceptor [2]catenanes and [2]rotaxanes used[9] in the construction of devices. These values are important for creating operating devices based on bistable mechanically interlocked compounds and suggest that it may be possible to use electrochemically switchable diastereoisomerism as the operational mechanism for a device in the future. Additionally, optically active pretzelanes could provide the means to create electrochemically controllable chiroptical switches.

Experimental Section

6: A mixture of the carboxylic acid derivative **5**[19] (0.50 g, 0.79 mmol), diethylene glycol (0.42 g, 3.97 mmol), 1,3-dicyclohexylcarbodiimide (DCC) (0.33 g, 1.59 mmol), and 4-(dimethylamino)pyridine (DMAP) (cat. amount) in CH_2Cl_2 (20 mL) was stirred for 1 h at room temperature. The resulting suspension was filtered, the filtrate was evaporated, and the residue was subjected to column chromatography (SiO_2:CH_2Cl_2/MeOH 30:1) to give the alcohol **6** (0.54 g, 95%). ^{1}H NMR (CD_3OD, 600 MHz, 298 K): δ 7.82 (d, J = 8.4 Hz, 2 H), 7.29 (t, J = 8.4 Hz,

(27) (a) Sutherland, I. O. *Annu. Rep. NMR Spectrosc.* **1971**, *4*, 71−235. (b) *Dynamic NMR Spectroscopy*; Sandstrom, J., Ed.; Academic Press: New York, 1982; Chapter 6.

(28) (a) Mann, B. E. *J. Magn. Reson.* **1976**, *21*, 17−23. (b) Mann, B. E. *J. Magn. Reson.* **1977**, *25*, 91−94. (c) Mann, B. E. *Prog. NMR Spectrosc.* **1977**, *11*, 95−114. (d) Perrin, C. L.; Johnston, E. R. *J. Magn. Reson.* **1979**, *33*, 619−626. (e) Perrin, C. L.; Johnston, E. R. *J. Am. Chem. Soc.* **1979**, *101*, 4753−4754.

(29) Binsch, G.; Kessler, H. *Angew. Chem., Int. Ed. Engl.* **1980**, *19*, 411−428.

2 H), 7.09 (d, J = 2.2 Hz, 2 H), 6.80 (d, J = 7.8 Hz, 2 H), 6.41 (t, J = 2.2 Hz, 1 H), 4.45 (t, J = 4.5 Hz, 2 H), 4.20 (t, J = 4.5 Hz, 4 H), 3.96 (t, J = 4.5 Hz, 4 H), 3.84−3.81 (m, 6 H), 3.77−3.76 (m, 4 H), 3.70−3.68 (m, 8 H), 3.67−3.65 (m, 4 H), 3.63−3.61 (m, 6 H), 3.33 (m, 2 H). ^{13}C NMR (CD_3OD, 150 MHz, 298 K): δ 166.3, 159.9, 154.3, 131.6, 126.7, 124.8, 114.2, 107.7, 105.5, 105.4, 72.4, 70.5, 70.5, S3 70.4, 70.3, 69.4, 69.2, 68.8, 67.8, 67.4, 64.2, 60.8. MS (ESI): 719.4 $[M + H]^+$, 741.3 $[M + Na]^+$, 757.2 $[M + K]^+$.

7: A mixture of the carboxylic acid derivative **5**[19] (0.40 g, 0.63 mmol), 1,4-butandiol (0.29 g, 3.17 mmol), DCC (0.16 g, 0.76 mmol), and DMAP (cat. amount) in CH_2Cl_2 (20 mL) was stirred for 1 h at room temperature. The resulting suspension was filtered, the filtrate was evaporated, and the residue was subjected to column chromatography (SiO_2:EtOAc/hexanes 1:1) to give the alcohol **7** (0.31 g, 69%). ^{1}H NMR ($CDCl_3$, 500 MHz, 298 K): δ 7.87 (d, J = 8.4 Hz, 2 H), 7.32 (t, J = 8.0 Hz, 2 H), 7.14 (d, J = 2.3 Hz, 2 H), 6.78 (d, J = 7.6 Hz, 2 H), 6.45 (t, J = 2.3 Hz, 1 H), 4.33 (t, J = 7.5 Hz, 2 H), 4.26 (t, J = 4.5 Hz, 4 H), 4.00 (t, J = 4.5 Hz, 4 H), 3.89 (t, J = 4.5 Hz, 4 H), 3.81 (t, J = 4.5 Hz, 4 H), 3.73−3.66 (m, 18 H), 2.20 (br s, 1 H), 1.84 (m, 2 H), 1.72 (m, 2 H). ^{13}C NMR (CD_3OD, 150 MHz, 298 K): δ 166.2, 159.6, 154.2, 131.8, 126.6, 125.0, 114.5, 107.5, 107.9, 105.8, 105.6, 70.9, 70.8, 70.7, 70.6, 69.6, 69.3, 68.0, 67.5, 64.8, 62.1, 29.0, 25.0. HRMS (MALDI) $C_{37}H_{50}O_{13}$: $[M + Na]^+$, calcd 725.3144, found 725.3163; $[M + K]^+$, calcd 741.2883, found 741.2900.

9: A mixture of the alcohol **6** (0.50 g, 0.70 mmol), the carboxylic acid derivative **8**[20] (0.30 g, 0.77 mmol), DCC (0.22 g, 1.0 mmol), and DMAP (cat. amount) in CH_2Cl_2 (20 mL) was stirred for 1 h at room temperature. The resulting suspension was filtered, the filtrate was evaporated, and the residue was subjected to column chromatography (SiO_2:hexanes/EtOAc 1:3) to give the dibromide **9** as a sticky solid (0.57 g, 75%). ^{1}H NMR (CDCl3, 500 MHz, 298 K): δ 7.83 (d, J = 8.4 Hz, 2 H), 7.69 (s, 2 H), 7.29 (t, J = 8.4 Hz, 2 H), 7.14 (d, J = 2.2 Hz, 2 H), 6.76 (d, J = 7.8 Hz, 2 H), 6.43 (t, J = 2.2 Hz, 1 H), 4.92 (s, 4 H), 4.44 (s, 2 H), 4.43 (t, J = 4.5 Hz, 2 H), 4.30 (t, 2 H), 4.25 (t, J = 4.5 Hz, 4 H), 3.98 (m, 6 H), 3.88 (t, J = 4.5 Hz, 4 H), 3.80−3.78 (m, 4 H), 3.76−3.74 (m, 2 H), 3.72−3.62 (m, 16 H). ^{13}C NMR ($CDCl_3$, 125 MHz, 298 K): δ 167.0, 166.4, 166.1, 159.6, 154.2, 137.0, 136.5, 129.7, 128.3, 127.9, 126.6, 125.0, 114.5, 108.1, 105.6, 70.9, 70.8, 70.7, 70.6, 69.6, 69.4, 69.1, 69.1, 68.0, 67.5, 64.8, 64.0, 33.9, 25.5. MS (ESI): 1114.5 $[M + Na]^+$, 1130.5 $[M + K]^+$.

10: A mixture of the alcohol **7** (0.12 g, 0.17 mmol), the carboxylic acid derivative **8**[20] (79 mg, 0.21 mmol), DCC (42 mg, 0.21 mmol), and DMAP (cat. amount) in CH_2Cl_2 (5 mL) was stirred for 1 h at room temperature. The resulting suspension was filtered, the filtrate was evaporated, and the residue was subjected to column chromatography (SiO_2:EtOAc/hexanes 3:1) to give the dibromide **10** as an oil (78 mg, 43%). ^{1}H NMR ($CDCl_3$, 500 MHz, 298 K): δ 7.83 (d, J = 8.4 Hz, 2 H), 7.65 (s, 2 H), 7.26 (t, J = 8.1 Hz, 2 H), 7.08 (d, J = 2.3 Hz, 2 H), 6.75 (d, J = 7.8 Hz, 2 H), 6.41 (t, J = 2.3 Hz, 1 H), 4.90 (s, 4 H), 4.42 (s, 2 H), 4.28 (br s, 2 H), 4.23 (m, 6 H), 3.96 (t, J = 4.5 Hz, 4 H), 3.85 (t, J = 4.5 Hz, 4 H), 3.77 (t, J = 4.5 Hz, 4 H), 3.70 (m, 4 H), 3.69−3.66 (m, 8 H), 3.64−3.62 (m, 4 H), 1.80 (m, 4 H). ^{13}C NMR ($CDCl_3$, 125 MHz, 298 K): δ 167.0, 166.4, 166.1, 159.6, 154.2, 137.1, 136.5, 131.6, 128.3, 126.6, 125.0, 114.5, 107.9, 105.9,105.6, 70.9, 70.8, 70.7, 70.6, 69.6, 69.4, 68.0, 67.5, 65.4, 64.3, 60.3, 38.7, 25.7, 25.2, 25.1, 14.1. HRMS (MALDI) $C_{49}H_{57}Br_2NO_{16}$: $[M + Na]^+$, calcd 1096.1936, found 1096.1963.

13: A solution containing 1.4 g (2.4 mmol) of **12**[22] in CH_2Cl_2 (60 mL) was prepared. Diethylene glycol (1.28 g, 12 mmol) and a catalytic amount of DMAP, followed by 0.94 g (4.8 mmol) of DCC, were added to this solution. This mixture was stirred for 3 h before being filtered, evaporated, and subjected to column chromatography (SiO_2:MeOH/CH_2Cl_2 5:95). The alcohol **13** was obtained as a clear oil (1.1 g, 69%). ^{1}H NMR (CD_2Cl_2, 500 MHz, 298 K): δ 2.00 (t, J = 6.2 Hz, 1 H), 3.57−3.80 (m, 30 H), 4.00 (dd, J = 4.4, 6.1 Hz, 4 H), 4.04 (dd, J = 4.4, 6.1 Hz, 4 H), 4.41 (dd, J = 4.4, 6.1 Hz, 2 H), 6.64 (t, J = 2.6 Hz, 1 H), 6.77 (s, 4 H), 7.15 (d, J = 2.6 Hz, 2 H). ^{13}C NMR (CD_2Cl_2, 150 MHz, 298 K): δ 61.7, 64.25, 67.9, 68.2, 69.1, 69.5, 69.7, 70.7, 70.7, 70.7, 70.8, 72.5, 106.1, 108.0, 115.6, 132.0, 153.0, 160.0, 166.1. HRMS (MALDI): *m/z* calcd for $C_{33}H_{48}O_{14}$-Na $[M + Na]^+$ 691.2936, found 691.2930.

14: A solution containing 0.55 g (0.82 mmol) of **13** in CH_2Cl_2 (20 mL) was prepared. Compound **8**[20] (0.35 g, 0.90 mmol) and a catalytic amount of DMAP, followed by 0.25 g (1.3 mmol) of DCC, were added to this solution. This mixture was stirred for 4 h under Ar, before being filtered, evaporated, and subjected to column chromatography (SiO_2:MeOH/CH_2Cl_2 5:95). The dibromide **14** was obtained as a sticky yellow solid (278 mg, 35%). ^{1}H NMR (CD_2Cl_2, 500 MHz, 298 K): δ 3.57−3.65 (m, 16 H), 3.71−3.79 (m, 12 H), 4.00 (dd, J = 4.4, 6.1 Hz, 4 H), 4.04 (dd, J = 4.4, 6.1 Hz, 4 H), 4.30 (dd, J = 4.4, 6.1 Hz, 2 H), 4.38 (dd, J = 4.4, 6.1 Hz, 2 H), 4.42 (s, 2 H), 4.93 (s, 4 H), 6.63 (t, J = 2.2 Hz, 1 H), 6.77 (s, 4 H), 7.15 (d, J = 2.2 Hz, 2 H). ^{13}C NMR (CD_2Cl_2, 600 MHz, 298 K): δ 64.2, 65.0, 68.0, 68.3, 68.8, 69.1, 69.5, 69.7, 70.6, 70.7, 70.7, 70.8, 106.1, 108.1, 115.6, 120.0, 128.5, 132.0, 136.6, 137.3, 153.1, 157.0, 159.9, 166.0, 166.5, 167.2. HRMS (MALDI): *m/z* calcd for $C_{45}H_{55}O_{17}$-$NNaBr_2$ $[M + Na]^+$ 1062.1729, found 1062.1718.

(*S*)-17: A mixture of the crown ether **15**[30] (0.35 g, 0.56 mmol), the carboxylic acid (*S*)-**16**[31] (0.12 g, 0.56 mmol), DCC (0.17 g, 0.84 mmol), and DMAP (cat. amount) in CH_2Cl_2 (10 mL) was stirred for 1 h at room temperature. The resulting suspension was filtered, the filtrate was evaporated, and the residue was subjected to column chromatography (SiO_2:hexanes/EtOAc 1:3) to give (*S*)-**17** (0.40 g, 87%). $[\alpha]^{22}_D$ +5.6 (*c* 0.85, $CHCl_3$). ^{1}H NMR ($CDCl_3$, 500 MHz, 298 K): δ 7.85 (d, J = 8.5 Hz, 2 H), 7.30 (t, J = 8.1 Hz, 2 H), 6.76 (d, J = 7.6 Hz, 2 H), 6.43 (d, J = 2.2 Hz, 2 H), 6.20 (t, J = 2.2 Hz, 1 H), 4.97 (s, 2 H), 4.28 (m, 1 H), 4.25 (t, J = 4.5 Hz, 4 H), 4.12 (t, J = 4.5 Hz, 4 H), 3.98 (t, J = 4.5 Hz, 4 H), 3.85−3.78 (m, 4 H), 3.71−3.66 (m, 12 H), 3.64−3.63 (m, 4 H), 2.52 (dd, J = 7.6, 14.6 Hz, 1 H), 2.40 (dd, J = 5.4, 14.6 Hz, 1 H), 1.18 (d, J = 6.1 Hz, 3 H), 0.85 (s, 9 H), 0.049 (s, 3 H), 0.025 (s, 3 H). ^{13}C NMR ($CDCl_3$, 125 MHz, 298 K): δ 171.3, 159.9, 154.2, 137.7, 126.7, 125.0, 114.5, 106.7, 105.6, 100.6, 71.0, 70.8, 70.7, 70.6, 69.6, 69.5, 68.0, 67.2, 65.9, 65.7, 44.7, 25.6, 23.8, 17.8, −4.6, −5.1. HRMS (MALDI) $C_{43}H_{64}O_{13}Si$: $[M + Na]^+$, calcd 839.4008, found 839.4014.

(*S*)-18: (*S*)-**17** (0.32 g, 0.39 mmol) was dissolved in THF (5 mL) and a THF solution of tetrabutylammonium fluoride (TBAF) (0.5 mL, 1 M) was added at 0 °C. The mixture was stirred overnight at room temperature, followed by the addition of saturated NH_4Cl solution (10 mL). The product was extracted with CH_2Cl_2 (3 × 10 mL). The combined organic layer was evaporated, and the residue was subjected to column chromatography (SiO_2:EtOAc) to give (*S*)-**18** as a colorless oil (0.19 g, 70%). $[\alpha]^{22}_D$ +6.9 (*c* 2.45, $CHCl_3$). ^{1}H NMR ($CDCl_3$, 500 MHz, 298 K): δ 7.84 (d, J = 8.4 Hz, 2 H), 7.29 (t, J = 8.0 Hz, 2 H), 6.76 (d, J = 7.6 Hz, 2 H), 6.42 (d, J = 2.2 Hz, 2 H), 6.20 (t, J = 2.2 Hz, 1 H), 5.01 (d, J = 3.9 Hz, 2 H), 4.24 (t, J = 4.5 Hz, 4 H), 4.19 (m, 1 H), 3.97 (t, J = 4.5 Hz, 4 H), 3.83 (t, J = 4.5 Hz, 4 H), 3.79−3.77 (m, 4 H), 3.71−3.66 (m, 12 H), 3.64−3.62 (m, 4 H), 2.97 (br s, 1 H), 2.53−2.42 (m, 2 H), 1.20 (d, J = 6.3 Hz, 3 H). ^{13}C NMR ($CDCl_3$, 125 MHz, 298 K): δ 172.5, 159.9, 154.2, 137.4, 126.7, 125.0, 114.5, 106.6, 105.6, 100.7, 70.9, 70.8, 70.7, 70.6, 69.6, 69.4, 68.0, 67.3, 66.1, 64.1, 42.7, 22.4. HRMS (MALDI) $C_{37}H_{50}O_{13}$: $[M + Na]^+$, calcd 725.3144, found 725.3113.

(*S*)-19: A mixture of the alcohol (*S*)-**18** (0.15 g, 0.21 mmol), the carboxylic acid derivative **8**[20] (89 mg, 0.23 mmol), DCC (64 mg, 0.31 mmol), and DMAP (cat. amount) in CH_2Cl_2 (5

(30) Ashton, P. R.; Parsons, I. W.; Raymo, F. M.; Stoddart, J. F.; White, A. J. P.; Williams, D. J.; Wolf, R. *Angew. Chem., Int. Ed. Engl.* **1998**, *37*, 1913−1916.

(31) Kobayashi, Y.; Kumar, G. B.; Kurachi, T.; Acharya, H. P.; Yamazaki, T.; Kitazume, T. *J. Org. Chem.* **2001**, *66*, 2011−2018.

mL) was stirred for 1 h at room temperature. The resulting suspension was filtered, the filtrate was evaporated, and the residue was subjected to column chromatography (SiO_2:EtOAc) to give the dibromide (*S*)-**19** as a sticky solid (0.10 g, 45%). $[\alpha]^{22}_D$ −6.5 (*c* 1.20, $CHCl_3$). ^1H NMR ($CDCl_3$, 500 MHz, 298 K): δ 7.83 (d, J = 8.5 Hz, 2 H), 7.67 (s, 2 H), 7.27 (t, J = 8.1 Hz, 2 H), 6.74 (d, J = 7.6 Hz, 2 H), 6.43 (d, J = 2.2 Hz, 2 H), 6.20 (t, J = 2.2 Hz, 1 H), 5.36 (m, 1 H), 5.01 (s, 2 H), 4.92 (s, 4 H), 4.34 (d, J = 2.4 Hz, 2 H), 4.23 (t, J = 4.5 Hz, 4 H), 3.97 (t, J = 4.5 Hz, 4 H), 3.84 (t, J = 4.5 Hz, 4 H), 3.78−3.76 (m, 4 H), 3.70−3.65 (m, 12 H), 3.63−3.62 (m, 4 H), 2.68 (dd, J = 7.5, 15.7 Hz, 1 H), 2.55 (dd, J = 5.7, 15.7 Hz, 1 H), 1.33 (d, J = 6.7 Hz, 3 H). ^{13}C NMR ($CDCl_3$, 125 MHz, 298 K): δ 169.4, 166.3, 166.2, 159.9, 154.2, 137.5, 137.0, 136.4, 128.3, 126.6, 125.0, 114.5, 106.7, 105.7, 100.7, 70.9, 70.8, 70.7, 70.6, 69.6, 69.4, 69.2, 68.0, 67.3, 66.3, 40.5, 38.8, 25.7, 19.7. HRMS (MALDI) $C_{49}H_{57}Br_2NO_{16}$: $[M + Na]^+$, calcd 1096.1936, found 1096.1984**.**

1·4PF$_6$: A solution of **9** (0.45 g, 0.41 mmol) and the dicationic salt **11**·2PF$_6$[21] (0.39 g, 0.55 mmol) in DMF (10 mL) was stirred at room temperature for 5 days. Diethyl ether (200 mL) was added to the reaction mixture to ensure precipitation of the crude product. The precipitate was isolated by vacuum filtration and subjected to column chromatography on silica gel (MeOH/aqueous NH_4Cl (2 M)/$MeNO_2$, 7:2:1). Purple fractions containing the product were combined and concentrated. Solid NH_4PF_6 was added to the residue to precipitate **1**·4PF$_6$ as a purple solid (0.39 g, 49%). Mp 195°C dec. ^1H NMR (CD_3CN, 500 MHz, 298 K): δ 9.27 (d, J = 6.6 Hz, 1 H), 9.19 (d, J = 6.6 Hz, 1 H), 8.88 (d, J = 6.6 Hz, 1 H), 8.73 (d, J = 6.6 Hz, 1 H), 8.65−8.59 (m, 3 H), 8.54 (d, J = 8.3 Hz, 1 H), 8.43 (d, J = 8.3 Hz, 1 H), 8.05 (d, J = 8.1 Hz, 1 H), 8.00−7.92 (m, 3 H), 7.43 (dd, J = 8.1, 2.4 Hz, 1 H), 7.41 (dd, J = 8.1, 2.4 Hz, 1 H), 7.38 (dd, J = 8.1, 2.4 Hz, 1 H), 7.36 (dd, J = 8.1, 2.4 Hz, 1 H), 7.28 (dd, J = 8.1, 2.4 Hz, 1 H), 7.27 (dd, J = 8.1, 2.4 Hz, 1 H), 7.00 (dd, J = 8.1, 2.4 Hz, 1 H), 6.95 (t, J = 1.5 Hz, 1 H), 6.81 (t, J = 1.5 Hz, 1 H), 6.67 (d, J = 13.7 Hz, 1 H), 6.62−6.60 (m, 2 H), 6.29 (d, J = 7.9 Hz, 1 H), 6.24 (d, J = 7.9 Hz, 1 H), 6.02 (t, J = 7.9 Hz, 1 H), 5.91−5.85 (m, 3 H), 5.78−5.73 (m, 4 H), 5.71 (t, J = 1.5 Hz, 1 H), 5.61 (t, J = 7.9 Hz, 1 H), 4.86 (d, J = 17.1 Hz, 1 H), 4.83 (dd, J = 12.5, 2.5 Hz, 1 H), 4.62 (dd, J = 12.5, 2.5 Hz, 1 H), 4.54 (d, J = 17.1 Hz, 1 H), 4.52−3.45 (m, 36 H), 3.29 (dd, J = 11.4, 2.5 Hz, 1 H), 3.07 (dd, J = 11.4, 2.5 Hz, 1 H), 2.50 (d, J = 8.1 Hz, 1 H), 2.44 ppm (d, J = 8.1 Hz, 1 H). MS(ESI): *m/z* 1783.4 $[M - PF_6]^+$, 818.9 $[M - 2PF_6]^{2+}$, 497.6 $[M - 3PF_6]^{3+}$. HRMS(ESI): *m/z* calcd for $C_{77}H_{81}N_5O_{17}P_3F_{18}$ $[M - PF_6]^+$ 1782.4547, found 1782.4559.

2·4PF$_6$: A mixture of the dibromide **10** (73 g, 68 μmol) and the dicationic salt **11**·2PF$_6$[21] (48 mg, 68 μmol) in DMF (3 mL) was stirred at room temperature for 5 days. The solvent was evaporated under reduced pressure and the residue was purified by column chromatography (SiO_2:MeOH/aqueous NH_4Cl (2 M)/$MeNO_2$ 7:2:1). The purple fractions containing the product were combined and concentrated to a residue. Solid NH_4PF_6 was added to precipitate **2**·4PF$_6$ as a purple solid (84 g, 65%). Mp 200 °C dec. ^1H NMR (CD_3CN, 500 MHz, 298 K): δ 9.38 (d, J = 6.6 Hz, 1 H), 9.20 (d, J = 6.6 Hz, 1 H), 8.83 (d, J = 6.6 Hz, 1 H), 8.70 (d, J = 6.6 Hz, 1 H), 8.65 (d, J = 6.6 Hz, 1 H), 8.63 (d, J = 6.6 Hz, 1 H), 8.59 (d, J = 6.6 Hz, 1 H), 8.53 (d, J = 8.3 Hz, 1 H), 8.41 (d, J = 8.3 Hz, 1 H), 8.00 (pseudo t, J = 10.0 Hz, 2 H), 7.93 (q, J = 8.3 Hz, 2 H), 7.75 (d, J = 6.6 Hz, 1 H), 7.43 (dd, J = 8.1, 2.4 Hz, 1 H), 7.37 (dd, J = 8.1, 2.4 Hz, 1 H), 7.33 (dd, J = 8.1, 2.4 Hz, 1 H), 7.30 (dd, J = 8.1, 2.4 Hz, 1 H), 7.23 (dd, J = 8.1, 2.4 Hz, 1 H), 7.17 (dd, J = 8.1, 2.4 Hz, 1 H), 6.99 (t, J = 1.5 Hz, 1 H), 6.91 (dd, J = 8.1, 2.4 Hz, 1 H), 6.88 (t, J = 1.5 Hz, 1 H), 6.61 (d, J = 13.7 Hz, 1 H), 6.55 (d, J = 13.7 Hz, 1 H), 6.24 (d, J = 7.9 Hz, 1 H), 6.19 (d, J = 7.9 Hz, 1 H), 6.16 (dd, J = 8.1, 2.4 Hz, 1 H), 5.91 (t, J = 7.9 Hz, 1 H), 5.86 (d, J = 13.7 Hz, 1 H), 5.85 (d, J = 13.7 Hz, 1 H), 5.79 (d, J = 13.7 Hz, 1 H), 5.74 (d, J = 7.9 Hz, 1 H), 5.72−5.67 (m, 3 H), 5.53 (t, J = 1.5 Hz, 1 H), 4.93 (m, 1 H), 4.89 (d, J = 17.1 Hz, 1 H), 4.60 (m, 1 H), 4.45−3.38 (m, 32 H), 3.26−3.24 (m, 1H), 3.18 (t, J = 8.7 Hz, 1 H), 2.70 (t, J = 8.7 Hz, 1 H), 2.41 (d, J = 8.1 Hz, 1 H), 2.36 (d, J = 8.1 Hz, 1 H). HRMS (ESI) $C_{77}H_{81}F_{24}N_5O_{16}P_4$: $[M - PF_6]^+$, calcd 1765.9559, found 1766.6005.

3·4PF$_6$: A solution containing 224 mg (0.22 mmol) of **14** and 159 mg (0.23 mmol) of **11**·2PF$_6$ in DMF (8 mL) was prepared. This mixture was stirred for two weeks before being evaporated and subjected to column chromatography (SiO_2:MeOH/aqueous NH_4Cl (2 M)/$MeNO_2$ 7:2:1). The chloride salt was then isolated from the column by evaporation and dissolved in H_2O, and an excess of NH_4PF_6 was added. The pretzelane **3**·4PF$_6$ was obtained by filtration as an orange solid (103 mg, 25%). Mp 200 °C dec; ^1H NMR (CD_3CN, 600 MHz, 235 K): δ 1.85 (dd, J = 3.2, 8.9 Hz, 1 H), 2.11 (dd, J = 2.9, 8.9 Hz, 1 H), 3.12 (t, J = 9.7 Hz, 1 H), 3.39 (t, J = 7.7 Hz, 1 H), 3.46 (dd, J = 5.3, 11.3 Hz, 1 H), 3.52−4.56 (m, 35 H), 4.62 (dd, J = 3.6, 10.9 Hz, 1 H), 4.68 (m, 1 H), 4.77 (d, J = 17 Hz, 1 H), 5.44 (dd, J = 2.8, 8.9 Hz, 1 H), 5.51 (dd, J = 3.2, 8.9 Hz, 1 H), 5.86−6.22 (m, 8 H), 6.60 (d, J = 13.7, 1 H), 6.87 (dd, J = 14.1 Hz, 1 H), 7.01 (d, J = 6.4 Hz, 2 H), 7.74−7.81 (m, 2 H), 7.92−8.04 (m, 4 H), 8.17−8.41 (m, 6 H), 8.59 (d, J = 8.2 Hz, 1 H), 8.64 (d, J = 6 Hz, 1 H), 8.80 (d, J = 8.2 Hz, 1 H), 9.11 (d, J = 6.5 Hz, 1 H), 9.40−9.47 (m, 4 H), 9.61 (d, J = 6.5 Hz, 1 H), 9.66 (d, J = 6.5 Hz, 1 H). HRMS (ESI): *m/z* calcd for $C_{73}H_{79}N_5O_{17}P_2F_{12}$ $[M - 2PF_6]^{2+}$ 793.7372, found 793.7351.

(*S*)-4·4PF$_6$: A solution of (*S*)-**19** (78 mg, 72 μmol) and the dicationic salt **11**·2PF$_6$[21] (51 mg, 72 μmol) in DMF (4 mL) was stirred at room temperature under 14 kbar for 3 days. The solvent was removed under reduced pressure and the residue was subjected to column chromatography (SiO_2:MeOH/aqueous NH_4Cl (2 M)/$MeNO_2$ 7:2:1). The purple fractions containing the product were combined and concentrated. Solid NH_4PF_6 was added to the residue to precipitate (*S*)-**4**·4PF$_6$ as a purple solid (38 mg, 27%). Mp.228 °C dec. ^1H NMR of the major diastereoisomer (*S*)-(*pS*)-(*P*)-(*M*)-**4**·4PF$_6$ (CD_3COCD_3, 500 MHz, 298 K): δ 9.27 (d, J = 6.6 Hz, 1 H), 9.19 (d, J = 6.6 Hz, 1 H), 8.88 (d, J = 6.6 Hz, 1 H), 8.73 (d, J = 6.6 Hz, 1 H), 8.65−8.59 (m, 3 H), 8.54 (d, J = 8.3 Hz, 1 H), 8.43 (d, J = 8.3 Hz, 1 H), 8.05 (d, J = 8.1 Hz, 1 H), 8.00−7.92 (m, 3 H), 7.43 (dd, J = 8.1, 2.4 Hz, 1 H), 7.41 (dd, J = 8.1, 2.4 Hz, 1 H), 7.38 (dd, J = 8.1, 2.4 Hz, 1 H), 7.36 (dd, J = 8.1, 2.4 Hz, 1 H), 7.28 (dd, J = 8.1, 2.4 Hz, 1 H), 7.27 (dd, J = 8.1, 2.4 Hz, 1 H), 7.00 (dd, J = 8.1, 2.4 Hz, 1 H), 6.95 (t, J = 1.5 Hz, 1 H), 6.81 (t, J = 1.5 Hz, 1 H), 6.67 (d, J = 13.7 Hz, 1 H), 6.62−6.60 (m, 3 H), 6.29 (d, J = 7.9 Hz, 1 H), 6.24 (d, J = 7.9 Hz, 1 H), 6.02 (t, J = 7.9 Hz, 1 H), 5.91−5.85 (m, 3 H), 5.78−5.73 (m, 3 H), 5.71 (t, J = 1.5 Hz, 1 H), 5.61 (d, J = 7.9 Hz, 1 H), 4.86 (d, J = 17.1 Hz, 1 H), 4.83 (dd, J = 12.5, 2.5 Hz, 1 H), 4.62 (dd, J = 12.5, 2.5 Hz, 1 H), 4.54 (d, J = 17.1 Hz, 1 H), 4.52−3.45 (m, 32 H), 3.29 (dd, J = 11.4, 2.5 Hz, 1 H), 3.07 (dd, J = 11.4, 2.5 Hz, 1 H), 2.50 (d, J = 8.1 Hz, 1 H), 2.44 (d, J = 8.1 Hz, 1 H). MS (ESI): 1783.4 $[M - PF_6]^+$, 818.9 $[M - 2PF_6]^{2+}$, 497.6 $[M - 3PF_6]^{3+}$. HRMS (ESI) $C_{77}H_{81}F_{24}N_5O_{17}P_4$: $[M - PF_6]^+$ calcd 1554.1606, found 1554.1638.

Acknowledgment. This work is supported by the Defense Advanced Research Projects Agency (DARPA) and the National Science Foundation (NSF) under grants CHE-9974928, CHE-9986344, CHE-0092036, and DGE−0114443.

Supporting Information Available: General methods for synthesis and ^1H NMR spectra of compounds **7**, **10**, **13**, **14**, **2**·4PF$_6$, and **3**·4PF$_6$. This material is available free of charge via the Internet at http://pubs.acs.org.

JO051430G